Variational Bayes Color Deconvolution with a Total Variation Prior

Miguel Vega*, Javier Mateos†, Rafael Molina† and Aggelos K. Katsaggelos‡
*Depto. de Lenguajes y Sistemas Informáticos, University of Granada, Granada, Spain
Email: mvega@ugr.es
†Depto. de Ciencias de la Computación e I.A., University of Granada, Granada, Spain
Email: {jmd,rms}@decsai.ugr.es
‡Dept. of Electrical Engineering and Computer Science, Northwestern University, Evanston, IL, USA
Email: aggk@eecs.northwestern.edu

***Abstract*—In digital brightfield microscopy, tissues are usually stained with two or more dyes. Color deconvolution aims at separating multi-stained images into single stained images. We formulate the blind color deconvolution problem within the Bayesian framework. Our model takes into account the similarity to a given reference color-vector matrix and spatial relations among the concentration pixels by a total variation prior. It utilizes variational inference and an evidence lower bound to estimate all the latent variables. The proposed algorithm is tested on real images and compared with classical and state-of-the-art color deconvolution algorithms.**

***Index Terms*—Blind color deconvolution, histopathological images, variational Bayes, total variation**

I. Introduction

In digital brightfield microscopy, tissues are usually stained before digitization and evaluation by pathologists. Hematoxylin and eosin (H&E) are probably the most widely used combination of stains. Computer-Aided Diagnosis (CAD) systems usually use the amount of each stain absorbed by a sample to quantitatively determine the presence of cancerous cells in the tissue [1]. Color deconvolution (CD) is a computational technique to separate multi-stained images into a set of images, one for each stain.

Several CD methods have been proposed (see [2] for a recent review of classical and state-of-the-art CD methods). One of the first CD methods was proposed by Ruifrok *et al.* [3]. This is a supervised manual method where the stain color vectors are obtained by measuring the relative absorption of each stain in single-stained images. These vectors are then applied to all the images, disregarding the inter-slide variability, which may result in a poor separation. To tackle inter-slide variability several blind (unsupervised) methods have been proposed. The works in [1] and [4] used Non-negative Matrix Factorization (NMF) and SVD corrected for robustness, respectively, to separate H&E stained images. More recently, in [5] clustering techniques are used to estimate the stain color vectors. McCann *et al.* [6] extended the method in [4] by taking into account the interaction between eosin and hematoxylin. In [7], [8], the NMF method in [1] is extended by including different sparsity and regularization terms. Alsubaie *et al.* [9], following [10], proposed the use of ICA in the wavelet domain. In [11], [12] a Variational Bayesian model with Simiultaneous Autoregresive (SAR) prior on the concentrations was proposed. These methods reduce noise in the image but also tend to smooth the borders of the structures in the image. In this paper we extend the method in [11] by using a total variation (TV) prior instead of the SAR prior. TV prior reduces the noise in the images while preserving sharp edges and has been successfully used to tackle the solution of other inverse problems such as denoising [13], image restoration [14] or super-resolution [15].

The rest of the paper is organized as follows: in section II the problem of color deconvolution is mathematically formulated. Following the Bayesian modelling and inference, in section III we propose an automatic method for the estimation of the concentrations and the color-vector matrix. In section IV, the proposed method is evaluated in a set of H&E stained images and its performance is compared with other classical and state-of-the-art CD methods. Finally, section V concludes the paper.

This work was supported in part by the Spanish Ministerio de Economía y Competitividad under contract DPI2016-77869-C2-2-R and the Visiting Scholar Program at the University of Granada.

II. Problem Formulation

A stained histological specimen's slide digitized by a brightfield microscope is stored as an RGB color image of size $M \times N$ represented by the $MN \times 3$ matrix by stacking each color component into a $MN \times 1$ column vector

$$\mathbf{I} = \begin{bmatrix} i_{1R} & i_{1G} & i_{1B} \\ \vdots & \vdots & \vdots \\ i_{MNR} & i_{MNG} & i_{MNB} \end{bmatrix} = \begin{bmatrix} \mathbf{i}_{1,:}^{\mathrm{T}} \\ \vdots \\ \mathbf{i}_{MN,:}^{\mathrm{T}} \end{bmatrix} = \begin{bmatrix} \mathbf{i}_R & \mathbf{i}_G & \mathbf{i}_B \end{bmatrix}, \tag{1}$$

Each value i_{ic}, $c \in \{R, G, B\}$, of the image is the transmitted light across the slide. For diagnostic purposes, however, the interest is centered on the contribution of each stain to this value, which can be performed in the absorbency or *optical density* (OD) image. According to its definition, the OD for channel c of the slide, $\mathbf{y}_c \in \mathbb{R}^{MN \times 1}$, is $\mathbf{y}_c = -\log_{10}\left(\mathbf{i}_c / \mathbf{i}_c^0\right)$, where $\mathbf{i}_c^0$ denotes the incident light, and the division operation and $\log_{10}(\cdot)$ function are computed element-wise.

The observed OD image $\mathbf{Y} \in \mathbb{R}^{MN\times 3}$ is composed by the RGB OD channels, i.e., $\mathbf{Y} = [\ \mathbf{y}_R\ \mathbf{y}_G\ \mathbf{y}_B\ ]$. The monochromatic Beer-Lambert law, for a slide stained with n_s stains, establishes that

$$\mathbf{Y}^{\mathrm{T}} = \mathbf{M}\mathbf{C}^{\mathrm{T}} + \mathbf{N}^{\mathrm{T}}, \tag{2}$$

where $\mathbf{N}$ is a random matrix of size $MN \times 3$ with i.i.d. zero mean Gaussian components with variance β^{-1}, $\mathbf{C} \in \mathbb{R}^{MN\times n_s}$ is the stain concentration matrix

$$\mathbf{C} = \begin{bmatrix} c_{11} & \dots & c_{1n_s} \\ \vdots & \ddots & \vdots \\ c_{MN1} & \dots & c_{MNn_s} \end{bmatrix} = \begin{bmatrix} \mathbf{c}_{1,:}^{\mathrm{T}} \\ \vdots \\ \mathbf{c}_{MN,:}^{\mathrm{T}} \end{bmatrix} = \begin{bmatrix} \mathbf{c}_1 \dots \mathbf{c}_{n_s} \end{bmatrix}, \tag{3}$$

with the i-th row $\mathbf{c}_{i,:}^{\mathrm{T}} = (c_{i1}, \dots, c_{in_s})$, $i = 1, \dots, MN$, representing the contribution of the stains at the i-th $\mathbf{I}$ pixel value and the s-th column $\mathbf{c}_s = (c_{1s}, \dots, c_{MNs})^{\mathrm{T}}$, $s \in \{1, \dots, n_s\}$, representing the concentrations of the s-th stain, and $\mathbf{M} \in \mathbb{R}^{3\times n_s}$ is the normalized stains' specific color-vector matrix

$$\mathbf{M} = \begin{bmatrix} m_{R1} \dots m_{Rn_s} \\ m_{G1} \dots m_{Gn_s} \\ m_{B1} \dots m_{Bn_s} \end{bmatrix} = \begin{bmatrix} \mathbf{m}_{R,:}^{\mathrm{T}} \\ \mathbf{m}_{G,:}^{\mathrm{T}} \\ \mathbf{m}_{B,:}^{\mathrm{T}} \end{bmatrix} = \begin{bmatrix} \mathbf{m}_1 \dots \mathbf{m}_{n_s} \end{bmatrix}. \tag{4}$$

Each column $\mathbf{m}_s$ in matrix $\mathbf{M}$ is a unit $\ell 2$ norm stain color-vector containing the relative RGB color composition of the corresponding stain in the OD space.

Color Deconvolution is a technique that allows us to obtain the stain concentration matrix, $\mathbf{C}$, and the color-vector matrix, $\mathbf{M}$, from the observed optical densities, $\mathbf{Y}$. Accordingly to (2), the contribution of each stain to the observed OD image can be separately calculated from $\sum_{s=1}^{n_s} \mathbf{m}_s \mathbf{c}_s^{\mathrm{T}}$.

In the following section we use Bayesian modeling and inference to estimate both $\mathbf{C}$ and $\mathbf{M}$.

III. Bayesian Modelling and Inference

Following the degradation model in (2), we have

$$\begin{aligned} \mathrm{p}(\mathbf{Y}|\mathbf{C},\mathbf{M}) &= \prod_{i=1}^{MN} \mathrm{p}(\mathbf{y}_{i,:}|\mathbf{M},\mathbf{c}_{i,:}) \\ &= \prod_{i=1}^{MN} \mathcal{N}(\mathbf{y}_{i,:}|\mathbf{M}\mathbf{c}_{i,:}, \beta^{-1}\mathbf{I}_{3\times 3}) \\ &\propto \prod_{i=1}^{MN} \exp\left(-\frac{1}{2}\beta\|\mathbf{y}_{i,:} - \mathbf{M}\mathbf{c}_{i,:}\|^2\right). \end{aligned} \tag{5}$$

For each independent stain concentrations vector prior we adopt the TV function, that is,

$$\mathrm{p}(\mathbf{C}) = \prod_{s=1}^{n_s} \mathrm{p}(\mathbf{c}_s) \propto \prod_{s=1}^{n_s} \exp\left[-\alpha_s \mathrm{TV}(\mathbf{c}_s)\right], \tag{6}$$

with $\alpha_s > 0$. The TV function is defined for any $\mathbf{c}_s$, $s \in \{1, \dots, n_s\}$, as

$$\mathrm{TV}(\mathbf{c}_s) = \sum_{i=1}^{MN} \sqrt{(\Delta_i^h(\mathbf{c}_s))^2 + (\Delta_i^v(\mathbf{c}_s))^2}, \tag{7}$$

where the operators $\Delta_i^h(\mathbf{c}_s)$ and $\Delta_i^v(\mathbf{c}_s)$ correspond to, respectively, the horizontal and vertical first order differences at pixel i.

The color-vector matrix $\mathbf{M} = [\mathbf{m}_1, \dots, \mathbf{m}_{n_s}]$ is also unknown because it depends on many factors that include the staining procedures and microscopes. In [3], color-vectors for hematoxylin, eosin, and DAB stains were proposed. Although those standard color-vectors are not usually exact for each single image, they have been frequently used. In this paper we incorporate the similarity to a reference color-vector matrix $\underline{\mathbf{M}} = [\underline{\mathbf{m}}_1, \dots, \underline{\mathbf{m}}_{n_s}]$ into the prior model on $\mathbf{M}$, as

$$\mathrm{p}(\mathbf{M}) = \prod_{s=1}^{n_s} \mathrm{p}(\mathbf{m}_s) \propto \prod_{s=1}^{n_s} \gamma_s^{\frac{3}{2}} \exp\left(-\frac{1}{2}\gamma_s\|\mathbf{m}_s - \underline{\mathbf{m}}_s\|^2\right), \tag{8}$$

where γ_s, $s = 1, \dots, n_s$, controls our confidence on the accuracy of $\underline{\mathbf{m}}_s$.

With all these ingredients, the joint probability distribution for our problem is

$$\mathrm{p}(\mathbf{Y},\mathbf{C},\mathbf{M}) = \mathrm{p}(\mathbf{Y}|\mathbf{C},\mathbf{M})\,\mathrm{p}(\mathbf{C})\,\mathrm{p}(\mathbf{M}). \tag{9}$$

We will denote the set of all unknowns by $\Theta = \{\mathbf{c}_1, \dots, \mathbf{c}_{n_s}, \mathbf{m}_1, \dots, \mathbf{m}_{n_s}\}$ and assume that the parameters $\beta, \alpha_1, \dots, \alpha_{n_s}, \gamma_1, \dots, \gamma_{n_s}$ are given. Their estimation is left for future work.

Following the Bayesian paradigm, inference will be based on the posterior distribution $\mathrm{p}(\Theta|\mathbf{Y})$. However, this posterior $\mathrm{p}(\Theta|\mathbf{Y})$ is intractable. Therefore, we consider an approximation of $\mathrm{p}(\Theta|\mathbf{Y})$ by a simpler tractable distribution $\mathrm{q}(\Theta)$ following the variational methodology [16]. The distribution $\mathrm{q}(\Theta)$ will be found by minimizing the Kullback-Leibler (KL) divergence, given by [17], [18]

$$\mathbf{KL}\left(\mathrm{q}(\Theta)\,||\,\mathrm{p}(\Theta|\mathbf{Y})\right) = \int \mathrm{q}(\Theta)\log\frac{\mathrm{q}(\Theta)}{\mathrm{p}(\Theta,\mathbf{Y})}\,\mathrm{d}\Theta + \log\mathrm{p}(\mathbf{Y}), \tag{10}$$

which is always non-negative and equal to zero only when $\mathrm{q}(\Theta) = \mathrm{p}(\Theta|\mathbf{Y})$. In order to obtain a tractable approximation, the family of distributions $\mathrm{q}(\Theta)$ are restricted utilizing the mean field approximation [19] so that

$$\mathrm{q}(\Theta) = \prod_{s=1}^{n_s} \mathrm{q}(\mathbf{c}_s) \prod_{s=1}^{n_s} \mathrm{q}(\mathbf{m}_s). \tag{11}$$

However, the use of the TV prior for $\mathbf{C}$ makes the integral in (10) difficult to evaluate even with this factorization. Therefore, a majorization of the TV prior is utilized to find an upper bound of the KL divergence (or equivalently a lower bound of the evidence). First, for α_s, $\mathbf{c}_s$, and any $N-$dimensional vector $\mathbf{u}_s \in (R^+)^{MN}$, $s = 1, \dots, n_s$, we define

$$\mathcal{M}_s(\mathbf{c}_s,\mathbf{u}_s) = \exp\left[-\frac{\alpha_s}{2}\sum_{i=1}^{MN}\frac{(\Delta_i^h(\mathbf{c}_s))^2 + (\Delta_i^v(\mathbf{c}_s))^2 + u_{is}}{\sqrt{u_{is}}}\right]. \tag{12}$$

Now, using the following inequality for $w \geq 0$ and $z > 0$

$$\sqrt{wz} \leq \frac{w+z}{2} \Rightarrow \sqrt{w} \leq \frac{w+z}{2\sqrt{z}}, \tag{13}$$

we can write

$$\exp[-\alpha_s \mathrm{TV}(\mathbf{c}_s)] \geq \mathcal{M}_s(\mathbf{c}_s, \mathbf{u}_s), \tag{14}$$

for $s = 1, \ldots, n_s$. We define

$$\mathcal{M}(\mathbf{C}, \mathbf{U}) = \prod_s \mathcal{M}_s(\mathbf{c}_s, \mathbf{u}_s), \tag{15}$$

where $\mathbf{U} = [\mathbf{u}_1 \ldots \mathbf{u}_{n_s}]$ and then define $\mathrm{F}(\Theta, \mathbf{U}, \mathbf{Y}) = \mathrm{p}(\mathbf{Y}|\mathbf{C}, \mathbf{M})\mathcal{M}(\mathbf{C}, \mathbf{U})\mathrm{p}(\mathbf{M})$ to obtain

$$\log \mathrm{p}(\Theta, \mathbf{Y}) \geq \log \mathrm{F}(\Theta, \mathbf{U}, \mathbf{Y}). \tag{16}$$

Utilizing the lower bound $\mathrm{F}(\Theta, \mathbf{U}, \mathbf{Y})$ for the joint probability distribution in (10) we minimize $\mathbf{KL}\left(\mathrm{q}(\Theta) \,||\, \mathrm{F}(\Theta, \mathbf{U}, \mathbf{Y})\right)$ instead of $\mathbf{KL}\left(\mathrm{q}(\Theta) \,||\, \mathrm{p}(\Theta|\mathbf{Y})\right)$.

Let us now obtain the analytic expressions for each latent variable. In what follows we use $\Theta \backslash \theta$ to represent all the variables in Θ except θ and $\langle \cdot \rangle_{\mathrm{q}(\Theta \backslash \theta)}$ denotes the expected value calculated using the distribution $\mathrm{q}(\Theta \backslash \theta)$. We will remove subscripts in expected values when clear from the context.

A. Concentration Update

To estimate the s-th stain concentration, the mean field variational distribution approximation establishes that

$$\mathrm{q}(\mathbf{c}_s) \propto \exp \left\langle \log \mathrm{p}(\mathbf{Y}|\mathbf{C}, \mathbf{M}) + \log \mathcal{M}_s(\mathbf{c}_s, \mathbf{u}_s) \right\rangle_{\mathrm{q}(\Theta \backslash \mathbf{c}_s)}. \tag{17}$$

Utilizing

$$\mathbf{e}_{i,:}^{-s} = \mathbf{y}_{i,:} - \sum_{k \neq s} \langle c_{ik} \rangle \langle \mathbf{m}_k \rangle \ , \quad i = 1, \ldots, MN, \tag{18}$$

and

$$z_i^{-s} = \langle \mathbf{m}_s \rangle^{\mathrm{T}} \mathbf{e}_{i,:}^{-s}, \quad i = 1, \ldots, MN, \tag{19}$$

we can easily show that

$$\log \mathrm{q}(\mathbf{c}_s) = -\frac{\beta}{2} \left(-2\mathbf{c}_s^{\mathrm{T}} \mathbf{z}^{-s} + \| \mathbf{c}_s \|^2 \left\langle \| \mathbf{m}_s \|^2 \right\rangle \right) - \frac{\alpha_s}{2} (\mathbf{c}_s)^{\mathrm{T}} \left[(\Delta^h)^{\mathrm{T}} \mathbf{W}(\mathbf{u}) \Delta^h + (\Delta^v)^{\mathrm{T}} \mathbf{W}(\mathbf{u}) \Delta^v \right] \mathbf{c}_s + \text{const} \tag{20}$$

which produces $\mathrm{q}(\mathbf{c}_s) = \mathcal{N}(\mathbf{c}_s | \langle \mathbf{c}_s \rangle, \mathbf{\Sigma}_{\mathbf{c}_s})$, where

$$\mathbf{\Sigma}_{\mathbf{c}_s}^{-1} = \beta \left\langle \| \mathbf{m}_s \|^2 \right\rangle \mathbf{I}_{MN \times MN} + (\Delta^h)^{\mathrm{T}} \mathbf{W}(\mathbf{u}_s) \Delta^h + (\Delta^v)^{\mathrm{T}} \mathbf{W}(\mathbf{u}_s) \Delta^v \tag{21}$$

$$\langle \mathbf{c}_s \rangle = \beta \mathbf{\Sigma}_{\mathbf{c}_s} \mathbf{z}^{-s}. \tag{22}$$

Above Δ^h and Δ^v represent the convolution matrices associated with the first order horizontal and vertical differences, respectively, and $\mathbf{W}(\mathbf{u}_s)$ is a diagonal matrix of the form $\mathbf{W}(\mathbf{u}_s) = \mathrm{diag}(u_{is}^{-1/2})$, for $i = 1, \ldots, MN$. This matrix $\mathbf{W}(\mathbf{u}_s)$ can be interpreted as a spatial adaptivity matrix since it controls the amount of smoothing at each pixel location depending on the strength of the intensity variation at that pixel, as expressed by the horizontal and vertical intensity gradient.

B. Color-Vector Update

In a similar way, we calculate the distribution of $\mathbf{m}_s$,

$$\mathrm{q}(\mathbf{m}_s) \propto \exp \left\langle \log \mathrm{p}(\mathbf{Y}|\mathbf{C}, \mathbf{M}) + \log \mathrm{p}(\mathbf{M}) \right\rangle_{\mathrm{q}(\Theta \backslash \mathbf{m}_s)}. \tag{23}$$

Using (18), we now have

$$\log \mathrm{q}(\mathbf{m}_s) = -\frac{\beta}{2} \left(\| \mathbf{m}_s \|^2 \sum_{i=1}^{MN} \left\langle c_{is}^2 \right\rangle - 2\mathbf{m}_s^{\mathrm{T}} \sum_{i=1}^{MN} \langle c_{is} \rangle \mathbf{e}_{i,:}^{-s} \right) - \frac{1}{2} \gamma_s \| \mathbf{m}_s - \underline{\mathbf{m}}_s \|^2 + \mathrm{e}, \tag{24}$$

which produces

$$\mathrm{q}(\mathbf{m}_s) = \mathcal{N}(\mathbf{m}_s | \langle \mathbf{m}_s \rangle, \mathbf{\Sigma}_{\mathbf{m}_s}), \tag{25}$$

where

$$\mathbf{\Sigma}_{\mathbf{m}_s}^{-1} = \left(\beta \sum_{i=1}^{MN} \left\langle c_{is}^2 \right\rangle + \gamma_s \right) \mathbf{I}_{3 \times 3}, \tag{26}$$

$$\langle \mathbf{m}_s \rangle = \mathbf{\Sigma}_{\mathbf{m}_s} \left(\beta \sum_{i=1}^{MN} \langle c_{is} \rangle \mathbf{e}_{i,:}^{-s} + \gamma_s \underline{\mathbf{m}}_s \right). \tag{27}$$

Notice that $\langle \mathbf{m}_s \rangle$ may not be a unitary vector even if $\underline{\mathbf{m}}_s$ is. We can always replace $\langle \mathbf{m}_s \rangle$ by $\langle \mathbf{m}_s \rangle / \| \langle \mathbf{m}_s \rangle \|$ and $\mathbf{\Sigma}_{\mathbf{m}_s}$ by $\mathbf{\Sigma}_{\mathbf{m}_s} / \| \langle \mathbf{m}_s \rangle \|^2$. Notice also that $\left\langle c_{is}^2 \right\rangle$ can be calculated using (22) and $\left\langle \| \mathbf{m}_s \|^2 \right\rangle$ can be easily calculated from (27) resulting in

$$\sum_{i=1}^{MN} \left\langle c_{is}^2 \right\rangle = \sum_{i=1}^{MN} \langle c_{is} \rangle^2 + \mathrm{tr}(\mathbf{\Sigma}_{\mathbf{c}_s}), \tag{28}$$

$$\left\langle \| \mathbf{m}_s \|^2 \right\rangle = \| \langle \mathbf{m}_s \rangle \|^2 + \mathrm{tr}(\mathbf{\Sigma}_{\mathbf{m}_s}). \tag{29}$$

C. $\mathbf{U}$ Update

To estimate the $\mathbf{U}$ matrix, we need to solve

$$\hat{\mathbf{U}} = \arg\min_{\mathbf{U}} \mathbf{KL}\left(\mathrm{q}(\Theta) \,||\, \mathrm{F}(\Theta, \mathbf{U}, \mathbf{Y})\right), \tag{30}$$

which is equivalent, for each s in $\{1, \ldots, n_s\}$, to

$$\hat{\mathbf{u}}_s = \arg\min_{\mathbf{u}_s} - \left\langle \log \mathcal{M}_s(\alpha_s, \mathbf{c}_s, \mathbf{u}_s) \right\rangle_{\mathrm{q}(\mathbf{c}_s)} = \arg\min_{\mathbf{u}_s} \sum_{i=1}^{MN} \frac{\left\langle (\Delta_i^h(\mathbf{c}_s))^2 + (\Delta_i^v(\mathbf{c}_s))^2 \right\rangle + u_{is}}{\sqrt{u_{is}}}, \tag{31}$$

whose solution is given by

$$\hat{u}_{is} = \arg\min_{u_{is}} \frac{\left\langle (\Delta_i^h(\mathbf{c}_s))^2 + (\Delta_i^v(\mathbf{c}_s))^2 \right\rangle + u_{is}}{\sqrt{u_{is}}} = \left\langle \Delta_i^h(\mathbf{c}_s)^2 \right\rangle + \left\langle \Delta_i^v(\mathbf{c}_s)^2 \right\rangle. \tag{32}$$

D. Calculating the concentration covariance matrices

The matrix $\mathbf{\Sigma}_{\mathbf{c}_s}$ must be explicitly calculated to find its trace and also $\hat{u}_{is}$. However, since its calculation is very intense, we propose the following approximation of the covariance matrix. We first approximate $\mathbf{W}(\mathbf{u}_s)$ using

$$\mathbf{W}(\mathbf{u}_s) \approx z(\mathbf{u}_s)\mathbf{I}, \tag{33}$$

Algorithm 1 Variational Bayesian TV Blind CD

Require: Observed image $\mathbf{I}$, reference (prior) color-vector matrix $\underline{\mathbf{M}}$, β, α_s and γ_s, $\forall s = 1, \ldots, n_s$.

Obtain the observed OD image $\mathbf{Y}$ from $\mathbf{I}$ and set $\langle \mathbf{m}_s \rangle^{(0)} = \underline{\mathbf{m}_s}$, $\mathbf{\Sigma}_{\mathbf{m}_s}^{(0)} = \mathbf{0}$, $\mathbf{\Sigma}_{\mathbf{c}_s}^{(0)} = \mathbf{0}$, $\langle \mathbf{c}_s \rangle^{(0)}$, $\forall s = 1, \ldots, n_s$, from the matrix $\mathbf{C}$ obtained as $\mathbf{C}^{\mathrm{T}} = \underline{\mathbf{M}}^{+}\mathbf{Y}^{\mathrm{T}}$, with $\underline{\mathbf{M}}^{+}$ the Moore-Penrose pseudo-inverse of $\underline{\mathbf{M}}$, and $n = 0$.

while convergence criterion is not met **do**

1. Set $n = n + 1$.
2. Using $\langle \mathbf{c}_s \rangle^{(n-1)}$ and $\mathbf{\Sigma}_{\mathbf{c}_s}^{(n-1)}$, $\forall s \in \{1, \ldots, n_s\}$, update the new variational parameters $\hat{\mathbf{u}}_s^{(n)}$ from (32).
3. Using $\langle \mathbf{c}_s \rangle^{(n-1)}$, $\mathbf{\Sigma}_{\mathbf{c}_s}^{(n-1)}$ and $\langle \mathbf{m}_s \rangle^{(n-1)}$ update the color-vectors $\mathbf{\Sigma}_{\mathbf{m}_s}^{(n)}$ and $\langle \mathbf{m}_s \rangle^{(n)}$ from (26) and (27), $\forall s$.
4. Using $\langle \mathbf{m}_s \rangle^{(n)}$, $\mathbf{\Sigma}_{\mathbf{m}_s}^{(n)}$ and $\hat{\mathbf{u}}_s^{(n)}$ update the concentrations $\mathbf{\Sigma}_{\mathbf{c}_s}^{(n)}$ and $\langle \mathbf{c}_s \rangle^{(n)}$ from (21) and (22), $\forall s$.

end while

Output the color-vector $\hat{\mathbf{m}}_s = \langle \mathbf{m}_s \rangle^{(n)}$ and the concentrations $\hat{\mathbf{c}}_s = \langle \mathbf{c}_s \rangle^{(n)}$, $\forall s \in \{1, \ldots, n_s\}$.

where $z(\mathbf{u}_s)$ is calculated as the mean value of the diagonal values in $\mathbf{W}(\mathbf{u}_s)$, that is,

$$z(\mathbf{u}_s) = \frac{1}{MN} \sum_i \frac{1}{\sqrt{u_{is}}}. \tag{34}$$

We then use the approximation

$$\begin{aligned} &\mathbf{\Sigma}_{\mathbf{c}_s}^{-1} \approx \beta \left\langle \| \mathbf{m}_s \|^2 \right\rangle \mathbf{I}_{MN \times MN} \\ &+ \alpha z(\mathbf{u}_s)(\Delta^h)^{\mathrm{T}}(\Delta^h) + \alpha z(\mathbf{u}_s)(\Delta^v)^{\mathrm{T}}(\Delta^v) = \mathbf{B}. \end{aligned} \tag{35}$$

Note that the matrix $\mathbf{B}$ is a block circulant matrix with circulant blocks (BCCB), thus, computing its inverse can be very efficiently performed in the discrete Fourier domain.

Finally we have

$$\begin{aligned} &\left\langle \Delta_i^h(\mathbf{c}_s)^2 \right\rangle + \left\langle \Delta_i^v(\mathbf{c}_s)^2 \right\rangle = (\Delta_i^h(\langle \mathbf{c}_s \rangle))^2 + (\Delta_i^v(\langle \mathbf{c}_s \rangle))^2 \\ &\quad + \left\langle (\Delta_i^h(\mathbf{c}_s - \langle \mathbf{c}_s \rangle)^2 \right\rangle + \left\langle (\Delta_i^v(\mathbf{c}_s - \langle \mathbf{c}_s \rangle)^2 \right\rangle. \\ &\quad \approx (\Delta_i^h(\langle \mathbf{c}_s \rangle))^2 + (\Delta_i^v(\langle \mathbf{c}_s \rangle))^2 \\ &\quad + \frac{1}{MN} \mathrm{tr} \left[\mathbf{B}^{-1} \times \left((\Delta^h)^{\mathrm{T}}(\Delta^h) + (\Delta^v)^{\mathrm{T}}(\Delta^v) \right) \right]. \end{aligned} \tag{36}$$

E. Proposed Algorithm

Based on the previous derivations, we propose the Variational Bayesian TV Blind Color Deconvolution in Algorithm 1. The linear equations problem in (22), used in step 4 of Alg. 1, has been solved using the Conjugate Gradient approach. Finally, from Alg. 1, an RGB image of each separated stain, $\hat{\mathbf{I}}_s^{\mathrm{sep}}$, can be obtained as

$$(\hat{\mathbf{I}}_s^{\mathrm{sep}})^{\mathrm{T}} = \exp_{10}(-\hat{\mathbf{m}}_s \hat{\mathbf{c}}_s^{\mathrm{T}}). \tag{37}$$

IV. Experimental results

We compared the proposed approach with classical and state-of-the-art CD methods on the *Warwick Stain Separation Benchmark* (WSSB) in [9]. WSSB includes 24 H&E stained images of different types of tissue: breast, colon and lung. In [9], ground truth stain color-vector matrices, $\mathbf{M}_{GT}$, were manually selected based on biological structures. Given those color-vector matrices, ground truth concentrations were derived as $\mathbf{C}_{GT}^{\mathrm{T}} = \mathbf{M}_{GT}^{+}\mathbf{Y}^{\mathrm{T}}$. Their corresponding ground truth RGB separated images can be obtained from (37). Figure 1(a) shows an example of breast observed image whose ground truth RGB separated E-only and H-only images are depicted, respectively, in the left and right hand sides of Fig. 1(b).

We have obtained a reference value for the color-vector matrix $\mathbf{M}$, $\underline{\mathbf{M}}$, by selecting a single pixel containing mainly hematoxylin and another pixel containing mainly eosin from each type of tissue, breast, colon and lung. These reference color vectors have also been used by the method in [12]. In Alg. 1 the parameters β, α_s and γ_s $\forall s = 1, \ldots, n_s$, are assumed to be known and their values have been experimentally determined to be $\alpha_1 = 7$, $\alpha_2 = 17$, $\beta = 6000$ and $\gamma_1 = \gamma_2 = 10^{20}$. The stopping criterion $\| \langle \mathbf{c}_s \rangle^{(n)} - \langle \mathbf{c}_s \rangle^{(n-1)} \|^2 / \| \langle \mathbf{c}_s \rangle^{(n)} \|^2 < 10^{-4}$ for both stains, that is, $s = 1, 2$, was used for the proposed algorithm.

We have compared the proposed method against non-blind color deconvolution method in [3], the classical blind method in [4] and the recent methods in [6], [8], [9] and [12]. For all the competing algorithms, parameters were selected following the recommendations on the original paper or the reference software freely available. Comparison is performed numerically by calculating the *Peak Signal to Noise Ratio* (PSNR) and *Structural Similarity* (SSIM) [20] between the reconstructed H-only and E-only images and their corresponding ground truth images, as well as visually.

Table I shows the numerical results of applying the proposed Alg. 1 to the dataset. The figures of merit obtained for the proposed method are higher than all of the competing methods. The H and E separated images obtained using the proposed and the competitors methods for the breast observed H&E image in Fig. 1a are shown in Fig. 1c-h. Due to space constraints, results from the method in [6] are not shown since they were quite close to those provide by the method in [4]. The figure shows that the best results are obtained by the proposed method and those in [8], [11] although the proposed method and the method in [11] produce more detailed images than those obtained by [8] and the proposed method produces crisper images than [11].

V. Conclusions

A novel variational Bayesian blind color deconvolution algorithm for histological images has been developed. It takes into account the spatial relations between pixels, by means of a total variation prior model, as well as the similarity to a reference color-vector matrix. Variational inference and an evidence lower bound to estimate all the latent variables are used. Comparison with classical and recent methods demonstrated the superiority of the proposed method. Future work includes the automatic parameter estimation.

References

[1] A. Rabinovich, S. Agarwal *et al.*, "Unsupervised color decomposition of histologically stained tissue samples," in *NIPS*, 2004, pp. 667–674.

TABLE I
PSNR AND SSIM FOR THE DIFFERENT METHODS AND STAIN IMAGES OF THE WSSB DATASET [9].

Image	Stain	Method in [3]		Method in [4]		Method in [6]		Method in [8]		Method in [9]		Method in [12]		Proposed Method	
		PSNR	SSIM	PSNR	SSIM	PSNR	SSIM	PSNR	SSIM	PSNR	SSIM	PSNR	SSIM	PSNR	SSIM
Colon	H	22.27	0.8141	23.91	0.8095	24.72	0.9100	25.83	0.8851	21.11	0.7241	28.57	0.9542	**28.82**	**0.9554**
	E	20.70	0.7456	21.55	0.6365	21.87	0.7905	26.29	0.8904	21.94	0.8540	27.58	0.9139	**27.99**	**0.9260**
Breast	H	15.27	0.6215	26.24	0.9552	23.89	0.8748	25.46	0.9239	24.60	0.8068	28.81	0.9528	**29.74**	**0.9661**
	E	17.66	0.7644	23.62	0.9336	19.81	0.8663	27.68	0.9550	25.92	0.9380	26.60	0.9464	**27.24**	**0.9568**
Lung	H	22.47	0.7987	19.52	0.7389	26.88	0.9318	25.87	0.8912	20.62	0.5551	32.91	0.9763	**34.46**	**0.9871**
	E	22.05	0.7734	18.09	0.5088	24.15	0.8539	25.53	0.8195	23.95	0.8939	30.77	0.9306	**32.19**	**0.9549**
Mean	H	20.00	0.7448	23.22	0.8345	25.16	0.9022	25.72	0.9100	22.11	0.6953	30.10	0.9611	**31.01**	**0.9695**
	E	20.14	0.7611	21.08	0.6930	21.94	0.8369	26.50	0.8883	23.94	0.8953	28.32	0.9303	**29.14**	**0.9459**

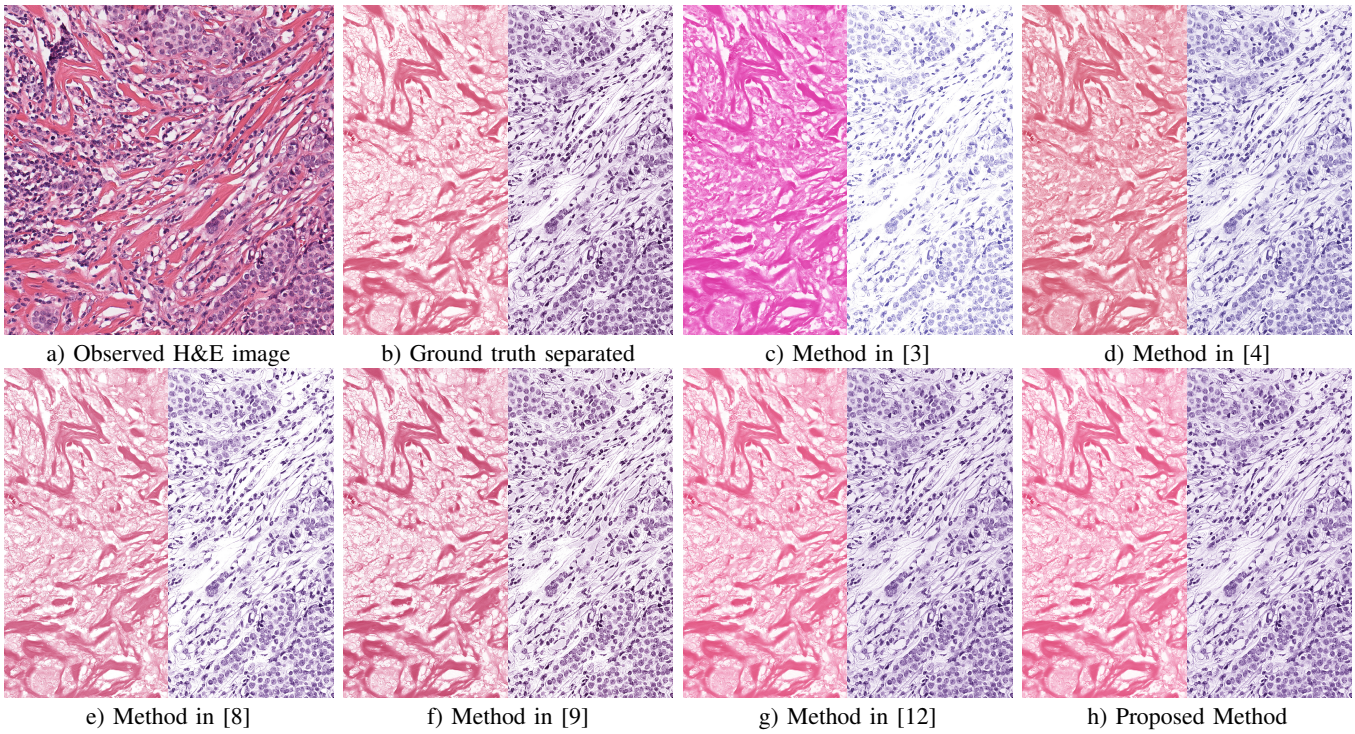

a) Observed H&E image b) Ground truth separated c) Method in [3] d) Method in [4]

e) Method in [8] f) Method in [9] g) Method in [12] h) Proposed Method

Fig. 1. Breast observed H&E image from the WSSB dataset in [9], its ground truth separated E-only and H-only images and results for the competing and proposed methods. Eosin and hematoxylin separations are presented on the left and right hand sides of each image, respectively.

[2] S. Roy, A. K. Jain *et al.*, "A study about color normalization methods for histopathology images," *Micron*, vol. 114, pp. 42–61, 2018.

[3] A. C. Ruifrok and D. A. Johnston, "Quantification of histochemical staining by color deconvolution," *Analytical and quantitative cytology and histology*, vol. 23, pp. 291–299, 2001.

[4] M. Macenko, M. Niethammer *et al.*, "A method for normalizing histology slides for quantitative analysis," in *ISBI*, 2009, pp. 1107–1110.

[5] M. Gavrilovic, J. C. Azar *et al.*, "Blind Color Decomposition of Histological Images," *IEEE Trans. on Medical Imaging*, vol. 32, pp. 983–994, 2013.

[6] M. T. McCann, J. Majumdar *et al.*, "Algorithm and benchmark dataset for stain separation in histology images," in *ICIP*, 2014, pp. 3953–3957.

[7] J. Xu, L. Xiang *et al.*, "Sparse non-negative matrix factorization (SNMF) based color unmixing for breast histopathological image analysis," *Computerized Medical Imaging and Graphics*, vol. 46, pp. 20–29, 2015.

[8] A. Vahadane, T. Peng *et al.*, "Structure-preserving color normalization and sparse stain separation for histological images," *IEEE Trans. on Medical Imaging*, vol. 35, pp. 1962–1971, 2016.

[9] N. Alsubaie, N. Trahearn *et al.*, "Stain deconvolution using statistical analysis of multi-resolution stain colour representation," *PLOS ONE*, vol. 12, p. e0169875, 2017.

[10] N. Trahearn, D. Snead *et al.*, "Multi-class stain separation using independent component analysis," in *Medical Imaging 2015: Digital Pathology*, 2015, p. 94200J.

[11] N. Hidalgo-Gavira, J. Mateos *et al.*, "Blind color deconvolution of histopathological images using a variational Bayesian approach," in *ICIP*, 2018, pp. 983–987.

[12] ——, "Fully automated blind color deconvolution of histopathological images," in *MICCAI*, 2018, pp. 183–191.

[13] M. Vega, J. Mateos *et al.*, "Bayesian TV denoising of SAR images," in *ICIP*, 2011, pp. 169–172.

[14] S. D. Babacan, R. Molina, and A. Katsaggelos, "Parameter estimation in TV image restoration using variational distribution approximation," *IEEE Trans. Image Processing*, pp. 326–339, 2008.

[15] D. Babacan, R. Molina, and A. Katsaggelos, "Total variation super resolution using a variational approach," in *ICIP*, 2008, pp. 641–644.

[16] M. Beal, "Variational algorithms for approximate Bayesian inference," Ph.D. dissertation, University College London, 2003.

[17] S. Kullback and R. A. Leibler, "On information and sufficiency," *Annals of Mathematical Statistics*, vol. 22, pp. 79–86, 1951.

[18] S. Kullback, *Information Theory and Statistics*. Dover Pub., 1959.

[19] G. Parisi, *Statistical Field Theory*. Addison-Wesley, 1988.

[20] Z. Wang, A. C. Bovik, and othersi, "Image quality assessment: from error visibility to structural similarity," *IEEE Trans. on Image Processing*, vol. 13, pp. 600–612, 2004.